Applied Physics Letters

$LaScO_3/SrTiO_3$: A conducting polar heterointerface of two *3d* band insulating perovskites

Cite as: Appl. Phys. Lett. **116**, 051603 (2020); https://doi.org/10.1063/1.5138718
Submitted: 18 November 2019 . Accepted: 23 January 2020 . Published Online: 04 February 2020

Sumit Kumar, Jyoti Kaswan, Biswarup Satpati, A. K. Shukla, Bhasker Gahtori, J. J. Pulikkotil, and Anjana Dogra

Applied Physics Letters ARTICLE scitation.org/journal/apl

$LaScO_3/SrTiO_3$: A conducting polar heterointerface of two *3d* band insulating perovskites

Cite as: Appl. Phys. Lett. **116**, 051603 (2020); doi: 10.1063/1.5138718
Submitted: 18 November 2019 · Accepted: 23 January 2020 ·
Published Online: 4 February 2020

Sumit Kumar,[1,2] Jyoti Kaswan,[1,2] Biswarup Satpati,[3] A. K. Shukla,[1,2] Bhasker Gahtori,[1,2] J. J. Pulikkotil,[1,2] and Anjana Dogra[1,2,a)]

AFFILIATIONS

[1]CSIR-National Physical Laboratory, Dr. K. S. Krishnan Road, New Delhi 110012, India
[2]Academy of Scientific and Innovative Research, CSIR-NPL Campus, New Delhi 110012, India
[3]Surface Physics and Material Science Division, Saha Institute of Nuclear Physics, Kolkata 700 064, India

[a)]anjanad@nplindia.org

ABSTRACT

This work reports a quasi-two-dimensional electron gas (q-2DEG) system at the interface of two wideband-gap insulators, (TiO_2-terminated) $SrTiO_3$ and $LaScO_3$, with a minimum thickness of 4-unit cell (uc). The highly crystalline and abrupt heterointerface is confirmed with high-resolution electron microscopy. The mixed Ti^{4+} and Ti^{3+} valence states (for 4 uc of $LaScO_3$) obtained from the x-ray photoelectron spectroscopy study suggest an intrinsic electronic reconstruction at the interface, leading to a metallic nature. This origin is well supported by density functional theory calculations that reveal an emergence of 3.3 states/eV/spin at the Fermi level for 4 uc in accordance with the polar catastrophe model. The study offers one more perovskite heterostructure, like $LaAlO_3/SrTiO_3$, for unraveling the q-2DEG phenomena toward a clear mechanism and futuristic applications.

The lattice symmetry breaking at the heterointerface of layered perovskite oxides leads to unique phenomena,[1–7] absent in individual layers. The most acknowledged example is the quasi two-dimensional electron gas (q-2DEG) with a very high carrier mobility at the interface of two wideband-gap insulators, $LaAlO_3$ (∼5.6 eV) and $SrTiO_3$ (∼3.2 eV).[1] This q-2DEG behavior, different from the strained semiconductor heterointerface, is attributed to the electronic reconstruction of Ti^{4+} into Ti^{3+} ions at the interface to minimize the electrostatic potential due to polar discontinuity between $(LaO)^+$ and $(TiO_2)^0$ layers; this is known as the polar catastrophe model. The discovery boosted an extensive research in polar perovskite $ABO_3/SrTiO_3$ heterointerfaces with different *3d* cations at the B-site. Interestingly, the heterointerface with $LaTiO_3$[8,9] and $LaVO_3$[10] shows metallicity, however, it remains insulating for $LaMnO_3$[11] and $LaCrO_3$.[12] It is observed that the d-cation charge reorganization for (Mn, Cr) cations lowers the electrostatic potential and hinders the q-2DEG state. Moreover, the insulting state in $LaTiO_3$ and $LaVO_3$ is of Mott-type (due to highly correlated *3d* electrons), which allows a weak insulting gap and minimal carrier mobility than the *3p* Al-based prototype $LaAlO_3$ system. It is shown that strain-mediated lattice distortion can suppress the weak Mott gap in $LaTiO_3$ (∼0.1 eV), showing an extrinsic 3D bulk transport; although for $LaVO_3$ (∼1.1 eV), the conduction is of 2D-type. Importantly, the conducting interface is not limited to polar oxides, but also reported for non-polar perovskites, e.g., lattice strain driven for $CaZrO_3$,[13] while extrinsic oxygen vacancy driven for $CaHfO_3$.[14] Thus, minimal structural imperfection may also lead to 3D bulk conductivity, either in the $SrTiO_3$ substrate by cation intermixing (doping) due to high energy plume kinematics or in the thin film from oxygen non-stoichiometry.

On the ground, the interface conductivity can be driven by both "intrinsic" polar discontinuity,[15] or strain-induced weak polarization[7] (2D transport) and "extrinsic" cation inter-diffusion[16] or oxygen vacancies[17–19] (3D transport). This puts the idealness of real samples as the primary condition for intrinsic 2D transport, followed by a wideband gap of two constituent oxides with a low lattice mismatch. Owing to this, *4p* Ga-based band insulators, $LaGaO_3$ (∼4.4 eV)[20] and $NdGaO_3$ (∼3.8 eV)[21] show q-2DEG transport similar to the *3p* Al-based prototype $LaAlO_3$ system, however, the low-stability of Gallium makes the growth complex for exploring a clear mechanism. In this work, we explore the *3d* Sc-based wideband gap insulator $LaScO_3$ (∼5.7 eV), and report, theoretically and experimentally, a "polar discontinuity"-driven q-2DEG system in the $LaScO_3/SrTiO_3$ heterostructure, quite analogous to the prototype *3p*-based $LaAlO_3/SrTiO_3$ system.

The structural and electronic properties of bulk $LaScO_3$ and $SrTiO_3$, and those of $LaScO_3/SrTiO_3$ heterostructures are studied by means of the full potential linearized augmented plane wave[22] (FP-LAPW) method as implemented in the WIEN2K suite of programs. The details of the calculations are provided in the supplementary material.

For the bulk $SrTiO_3$ and $LaScO_3$, the pseudo-cubic equilibrium lattice constant is determined as 3.94 Å and 4.07 Å, respectively, which are in good agreement with the experimental data, within 1% of error. From these parameters, it can be anticipated that the epitaxially grown $LaScO_3$ films would be compressively strained on the $SrTiO_3$ substrate with a lattice mismatch of 3.2%. Within similar approximations, the computed lattice constant of 3.82 Å for $LaAlO_3$ shows a tensile nature of the strain at the $LaAlO_3/SrTiO_3$ hetero-interface. Thus, these findings suggest that although $LaScO_3$ and $LaAlO_3$ are isoelectronic and isostructural systems, the $LaScO_3/SrTiO_3$ represents a compressively strained system, in contrast to the $LaAlO_3/SrTiO_3$, which is tensile strained.

Besides, the electronic bandgaps (Eg) of $SrTiO_3$, $LaScO_3$, and $LaAlO_3$ are computed to be 2.0 eV, 2.8 eV, and 3.6 eV, respectively. Thus, we find that Eg ($SrTiO_3$) < Eg ($LaScO_3$) < Eg ($LaAlO_3$). Note that, although the Eg values are considerably smaller than the experimental values, these values still serve as a good approximation in empirically suggesting that electrons will flow into the $SrTiO_3$ substrate from the $LaScO_3$ and $LaAlO_3$. The electronic structure of the structurally relaxed $LaScO_3/SrTiO_3$ heterostructure is described in terms of their layer resolved density of states (DOS) and band structure, as shown for two cases with 3 and 4 $LaScO_3$ MLs in Figs. 1(a) and 1(b), respectively. For 3 ML $LaScO_3/SrTiO_3$, the LaO/TiO_2 interface is insulating with a bandgap of 0.6 eV. The valence band spectra are dominated by the O *2p* states of the substrate, while the conduction band minimum (CBM) is dominated by the Ti *3d* states. The Sc *3d* states are ∼1 eV above the CBM. On the other hand, DOS spectra for 4 ML $LaScO_3/SrTiO_3$ show finite states at the Fermi energy, revealing a q-2DEG state. Importantly, the critical thickness of 4 MLs for the emergence of q-2DEG in $LaScO_3/SrTiO_3$ is identical to that for the $LaAlO_3/SrTiO_3$.[4] Furthermore, the layer resolved DOS reveals that the conducting carriers are derived from the Ti *3d* bands with confinement to nearly 2 MLs of $SrTiO_3$. The total DOS at Fermi energy is determined to be 3.3 states/eV/spin, of which the interface TiO_2 layer contributes ∼15% and the sub-interface TiO_2 layer has its contribution as ∼11%. The systematic downward shift in the Ti *3d* band of the $SrTiO_3$ substrate, due to the increasing built-up of the electrostatic potential in the $LaScO_3$ films, is however compensated by the upward shift of the O *2p* bands of $LaScO_3$. As evident from Fig. 1(b), the O *2p* bands of the surface ScO_2 layers therefore are introduced with holes. The very kind of charge transfer, from surface layers to the TiO_2 hetero-interface layers, is previously observed in the $LaAlO_3/SrTiO_3$ heterostructure, in line with the predictions of the polar catastrophe model.

To test the theoretical finding of q-2DEG in the $LaScO_3/SrTiO_3$ heterostructure, the epitaxial thin films of $LaScO_3$ with varying thickness (3–15 unit cell) are deposited on the (*001*) TiO_2-terminated $SrTiO_3$ single-crystal substrate by the pulsed laser deposition (PLD) technique with layer-by-layer growth monitoring by *in situ* reflection high-energy electron diffraction (RHEED). The details of the growth and characterization tools are provided in the supplementary section. Figure 2(a) shows the regular RHEED intensity oscillations for 4- and 15-unit cell (uc) thick films recorded *in situ* during the growth, which clearly exhibits the two-dimensional (2D) epitaxial growth of the $LaScO_3$. The 2D streaky RHEED pattern shown in the inset of Fig. 2(a) confirms the layer-by-layer growth for the $LaScO_3$ film with identical distance between two streaks to that for the $SrTiO_3$ substrate. Complimenting the RHEED results, the high-resolution x-ray diffraction (HRXRD) pattern for the thicker (∼40 nm) film shows only the (*00l*) reflections of the perovskite structure with the out-of-plane lattice parameter, c = 4.058 Å (see Fig. S1 in the supplementary material). Moreover, the surface analysis by atomic force microscopy for the 8 uc thick film reveals the persistence of similar terraces (see Fig. S2 in the supplementary material), as for the before-growth TiO_2-terminated surface of the $SrTiO_3$ substrate with approximately 0.39 nm step

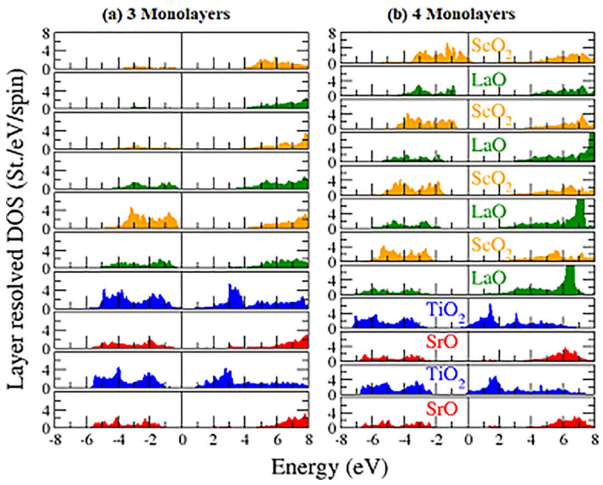

FIG. 1. The layer resolved density of states (DOS) for *the* $LaScO_3/SrTiO_3$ heterostructure with (a) 3 monolayers and (b) 4 monolayers of the $LaScO_3$ film.

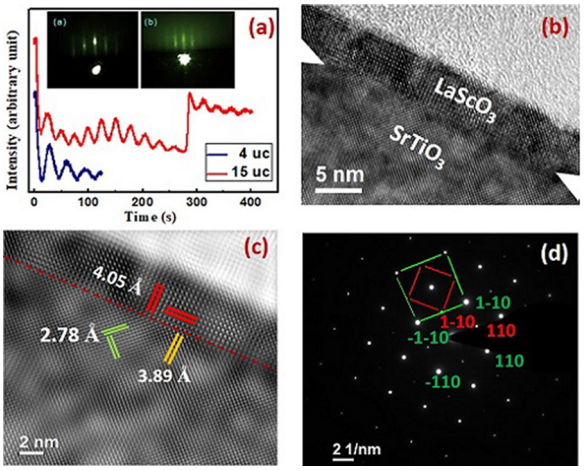

FIG. 2. (a) RHEED intensity oscillation during the growth of the thin film along with the RHEED pattern of the bare substrate (left) and thin film (right). (b) XTEM image of the 10 uc structure. (c) Fourier filtered XTEM image and (d) SAED pattern of the same structure and same image shown in (b).

height. This indicates that $LaScO_3$ adopts a pseudo-cubic symmetry over the $SrTiO_3$ substrate, giving an abrupt interface between two oxides. The interface quality is further examined for the 10 uc thick film with cross-sectional transmission electron microscopy (XTEM) along with the selected area electron diffraction (SAED) patterns. The XTEM on the 5 nm scale shows the clear boundary between the $SrTiO_3$ substrate and the $LaScO_3$ thin film with a thickness of 4.56 nm, as shown in Fig. 2(b). The Fourier filtered XTEM image for the same micrograph shows an atomically flat and coherent heterointerface with smooth relaxation in the thin film [see Fig. 2(c)], excluding any cation inter-diffusion between the substrate and thin film. The lattice parameter analysis by XTEM and SAED [see Fig. 2(d)] gives the single-domain and tetragonally strained $LaScO_3$ thin film with in-plane $a^* = 4.05$ Å, which is in well consistent with $a^* = 4.058$ Å from the HRXRD study.

The highly crystalline $LaScO_3/SrTiO_3$ interface is further subjected to sheet resistance measurement as a function of temperature, $R(T)$ from room temperature to 30 K. The heterointerface with $LaScO_3$ thickness ≥ 4 uc shows metallic behavior down to 30 K [see Fig. 3], which indicates the q-2DEG formation at the $LaScO_3/SrTiO_3$ heterointerface. The measured room temperature carrier concentration (n_s) of the order of 10^{13} cm^{-2} at the interface and the carrier mobility (μ_H) of 4–7 cm^2 V^{-1} s^{-1} (for 4–15 uc) from Hall measurement are almost similar to the prototype $LaAlO_3/SrTiO_3$.[1,23] Thus, considering the nearly equal bandgap and dielectric constant of $LaScO_3$ (~5.7 eV, 29) to $LaAlO_3$ (~5.6 eV, 25), at the first point, the observed interface conductivity in our heterointerface above critical thickness (i.e., $\geq$4 uc) can be attributed to the polar discontinuity between polar $(LaO)^+$ and non-polar $(TiO_2)^0$ layers, similar to $LaAlO_3/SrTiO_3$.[1,15]

Now, we discuss the possible origin mechanism of a conducting interface in transport measurements, considering both "intrinsic" polar discontinuity (2D transport) and "extrinsic" cation disorder and oxygen vacancies (3D transport). The foremost important thing is that our epitaxial thin film is grown with a laser fluence of ~1 J/cm^2, similar to $LaAlO_3$,[24] while it is significantly lower than for $LaTiO_3$,[8,9] $LaVO_3$,[10] $LaGaO_3$,[20] etc. to exclude the possibility of high energy La/Sc

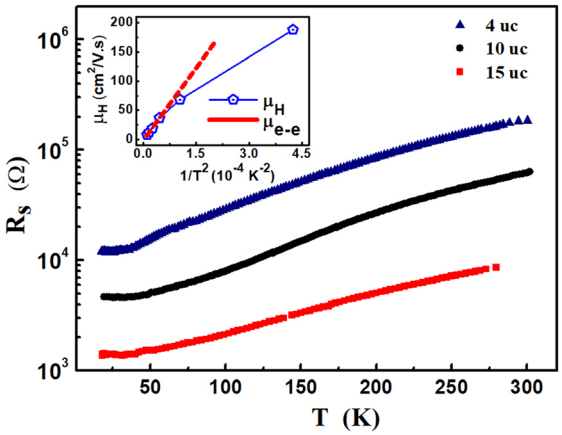

FIG. 3. The thermal variation of sheet resistance showing a metallic behavior. The inset shows the hall mobility of the 15 uc $LaScO_3/SrTiO_3$ structure plotted against $1/T^2$ with a high temperature linear variation (red line), corresponding to e-e (2D) interactions.

inter-diffusion (doping) to the $SrTiO_3$ substrate, which is further supported by the XTEM study. To exclude oxygen vacancies in the TiO_2-terminated $SrTiO_3$ substrate, the high insulating nature after annealing of the bare substrate at deposition conditions is verified before the growth. Furthermore, the $LaScO_3$ thin film deposition is performed in $p_{O2} \sim 10^{-4}$ mbar, similar to $LaAlO_3$,[25–27] which excludes any major contribution to interface conductivity from the oxygen vacancies. Moreover, on lowering of temperature from 300 K to 50 K, a minimal decrease in n_s ~9.4–4.7 × 10^{13} cm^{-2} suggests a 2D transport behavior (see Fig. S3 in the supplementary material). More importantly, the carrier mobility shows $1/T^2$ dependence at high temperatures (150 K–300 K) in accordance with electron–electron interactions at the 2D interface, a rather exponential increase for electron–phonon interactions in 3D transport.[25] At lower temperatures, the mobility shows a saturation-like behavior to the low-temperature limit with the highest carrier mobility of 1.88 × 10^2 cm^2 V^{-1} s^{-1} at 50 K. Thus, the transport measurements reveal the formation of q-2DEG state at the $LaScO_3/SrTiO_3$ heterointerface, primarily driven by "intrinsic" polar discontinuity in the system.

Here, we point out that the obtained n_s ~9.4–4.7 × 10^{13} cm^{-2} (for 10–15 uc) is significantly lower than the calculated charge transfers due to polar-discontinuity i.e., 0.5e$^-$/Ti or $n_s \simeq 3 \times 10^{14}$ cm^{-2} in the polar catastrophe model. The lower experimental n_s value can be directly associated with the presence of two kind of electrons, free (or mobile) as considered in the polar catastrophe scenario and second localized electrons either "intrinsically" in *3d*-based oxides or "extrinsically" trapped in defect states.[28] The presence of localized electrons reduces the effective charge transfer due to polar discontinuity. The picture of two kind "free" and "localized" charge carriers is well supported by Shubnikov-de Haas oscillations measurement.[29] Besides, as an alternative, Yu *et al.*[30] proposed that polar discontinuity is thermodynamically destabilized by the spontaneous formation of defects like oxygen vacancies leading to a conducting interface, while some of the oxygen vacancies are further compensated by anti-site pairs (cation disorder), thus, reducing the carrier density in comparison to that calculated from polar discontinuity.

The experimental existence of electrons which contribute to the conducting interface is analyzed by x-ray photoelectron spectroscopy (XPS). In Fig. 4, we compare the Ti *2p* core level spectra of 3 uc and 4 uc thick $LaScO_3$ films grown on TiO_2-terminated $SrTiO_3$. For non-conducting $LaScO_3$ (3 uc)/$SrTiO_3$, spin-orbit doublet peaks of Ti $2p_{3/2}$ and Ti $2p_{1/2}$ appear at 458.4 and 464.2 eV core level binding energy (BE), respectively, corresponding to the 4^+ charge state of Ti ions. In comparison, for the conducting $LaScO_3$ (4 uc)/$SrTiO_3$, peaks corresponding to Ti^{4+} appear at 0.1 eV higher BE compared to 3 uc $LaScO_3/SrTiO_3$. Besides, we can clearly observe the emergence of an extra well resolved feature at the lower BE side of the Ti $2p_{3/2}$ main peak of 4 uc $LaScO_3/SrTiO_3$. To quantify the peak parameters, energy position and the full width at half maximum (FWHM), we have performed χ^2 iterative fitting of the Ti $2p_{3/2}$ region using two components corresponding to the main peak and weaker intensity lower BE side feature. These fittings are shown in Fig. 4(b). The energy position of the lower BE feature [shaded region in Fig. 4(b)] is found to be separated by 1.9 eV from the main peak and such a feature has been attributed to the Ti^{3+} valence state.[3,31–38] This Ti^{3+} related feature, a consequence of the polar catastrophe induced electronic reconstruction of Ti ions at the interface, has been taken as the signature of quasi

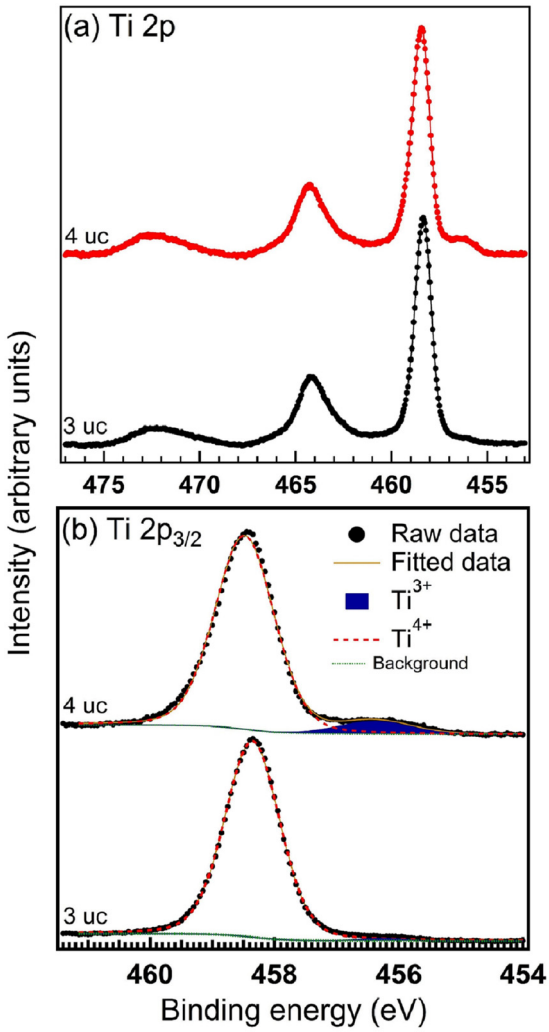

FIG. 4. (a) Ti 2p core-level photoemission spectra of the 3 uc and 4 uc $LaScO_3/SrTiO_3$. Spectra have been normalized at *the* highest peak and staggered vertically for clarity. (b) Ti 2p3/2 core-level photoemission spectra for 3 uc and 4 uc $LaScO_3/SrTiO_3$. Experimental spectra (open circles), fitted spectra (green solid line), deconvoluted components used to fit Ti^{4+} (red dashed line), and Ti^{3+} (blue shaded) along with the simulated Shirley background (pink dashed line) are also shown.

two-dimensional electron gas (q-2DEG) in polar/non-polar oxide heterostructures. The relative percentage (normalized peak area) of Ti^{3+} to Ti^{4+} has been estimated to be 6.8% for 4 uc $LaScO_3/SrTiO_3$, while it is negligible (0.85%) for 3 uc $LaScO_3/SrTiO_3$. Peak fittings revealed that the FWHM of the Ti $2p_{3/2}$ (Ti^{4+}) for 3 and 4 uc $LaScO_3/SrTiO_3$ turns out to be 1.05 and 1.15 eV, respectively. The shift of the Ti *2p* core level toward the higher BE side for the conducting interface (4 uc) and the increase in its FWHM compared to non-conducting 3 uc $LaScO_3/SrTiO_3$ can be the consequence of the band bending effect and it has also been considered as the evidence for the presence of q-2DEG in polar/non-polar systems.[32,33,37]

In summary, the highly crystalline $LaScO_3$ epitaxial thin films are grown on a (*001*) TiO_2-terminated $SrTiO_3$ substrate by the PLD technique with two-dimensional growth ensured by *in situ* RHEED. The abrupt interface quality with no substrate-film inter-diffusion is confirmed with the cross-sectional TEM study. The electric transport measurements reveal the formation of q-2DEG at the heterointerface for films with $LaScO_3$ thickness ≥ 4 uc, at room temperature carrier concentration of 10^{13} cm^{-2} at the interface, and a mobility of 4–7 cm^2 V^{-1} s^{-1}, quite similar to the prototype $LaAlO_3/SrTiO_3$ q-2DEG system. Finally, the XPS study reveals electronic reconstruction of Ti ions at the interface as a signature of the "Polar Catastrophe" origin of the q-2DEG state. On top of this, the DFT calculations show the emergence of q-2DEG in the $LaAlO_3/SrTiO_3$ heterostructure in accordance with the polar catastrophe model, in which the increasing electrostatic potential due to the increasing $LaScO_3$ film thickness transfers charge from the surface layer to the hetero-interface. Thus, the study provides a *3d* band-insulator based q-2DEG system, beyond the existing *3p*-based $LaAlO_3/SrTiO_3$, to explore futuristic quantum applications.

See the supplementary material which contains the theoretical calculations and experimental methods of the present study. Figs. S1 S3 illustrate the HRXRD, AFM, and Hall mobility measurement of the $LaScO_3/SrTiO_3$ heterostructure, respectively.

The authors are grateful to Director, NPL for his constant encouragement and support. A.D. and J.J.P. acknowledge the funding from DST (Project No. #EMR/2014/00/004). We thank H K Singh for his support while performing $R(T)$ measurement in his lab. S.K. is thankful to the CSIR (No. 31/001(0463)2016-EMR-I) for the fellowship.

REFERENCES

[1] A. Ohtomo and H. Y. Hwang, Nature **427**, 423 (2004).
[2] A. Brinkman, M. Huijben, M. van Zalk, J. Huijben, U. Zeitler, J. C. Maan, W. G. van der Wiel, G. Rijnders, D. H. A. Blank, and H. Hilgenkamp, Nat. Mater. **6**, 493 (2007).
[3] P. Kumar, P. Pal, A. K. Shukla, J. J. Pulikkotil, and A. Dogra, Phys. Rev. B **91**, 115127 (2015).
[4] A. Rastogi, J. J. Pulikkotil, S. Auluck, Z. Hossain, and R. C. Budhani, Phys. Rev. B **86**, 075127 (2012).
[5] D. A. Dikin, M. Mehta, C. W. Bark, C. M. Folkman, C. B. Eom, and V. Chandrasekhar, Phys. Rev. Lett. **107**, 056802 (2011).
[6] A. M. R. V. L. Monteiro, D. J. Groenendijk, I. Groen, J. de Bruijckere, R. Gaudenzi, H. S. J. van der Zant, and A. D. Caviglia, Phys. Rev. B **96**, 020504 (2017).
[7] G. N. Daptary, P. Kumar, A. Dogra, and A. Bid, Phys. Rev. B **98**, 035433 (2018).
[8] J. Biscaras, N. Bergeal, A. Kushwaha, T. Wolf, A. Rastogi, R. C. Budhani, and J. Lesueur, Nat. Commun. **1**, 89 (2010).
[9] F. J. Wong, S.-H. Baek, R. V. Chopdekar, V. V. Mehta, H.-W. Jang, C.-B. Eom, and Y. Suzuki, Phys. Rev. B **81**, 161101 (2010).
[10] Y. Hotta, T. Susaki, and H. Y. Hwang, Phys. Rev. Lett. **99**, 236805 (2007).
[11] J. Garcia-Barriocanal, F. Y. Bruno, A. Rivera-Calzada, Z. Sefrioui, N. M. Nemes, M. Garcia-Hernández, J. Rubio-Zuazo, G. R. Castro, M. Varela, S. J. Pennycook, C. Leon, and J. Santamaria, Adv. Mater. **22**, 627 (2010).
[12] R. Colby, L. Qiao, K. H. L. Zhang, V. Shutthanandan, J. Ciston, B. Kabius, and S. A. Chambers, Phys. Rev. B **88**, 155325 (2013).
[13] Y. Chen, F. Trier, T. Kasama, D. V. Christensen, N. Bovet, Z. I. Balogh, H. Li, K. T. S. Thydén, W. Zhang, S. Yazdi, P. Norby, N. Pryds, and S. Linderoth, Nano Lett. **15**, 1849 (2015).
[14] M. Zhang, K. Du, T. Ren, H. Tian, Z. Zhang, H. Y. Hwang, and Y. Xie, Nat. Commun. **10**, 4026 (2019).
[15] S. Thiel, Science **313**, 1942 (2006).

[16]N. Nakagawa, H. Y. Hwang, and D. A. Muller, Nat. Mater. **5**, 204 (2006).
[17]A. H. Al-Tawhid, J. R. Frick, D. B. Dougherty, and D. P. Kumah, J. Vac. Sci. Technol., A **37**, 021102 (2019).
[18]N. C. Bristowe, P. B. Littlewood, and E. Artacho, Phys. Rev. B **83**, 205405 (2011).
[19]G. Herranz, M. Basletić, M. Bibes, C. Carrétéro, E. Tafra, E. Jacquet, K. Bouzehouane, C. Deranlot, A. Hamzić, J.-M. Broto, A. Barthélémy, and A. Fert, Phys. Rev. Lett. **98**, 216803 (2007).
[20]P. Perna, D. Maccariello, M. Radovic, U. Scotti di Uccio, I. Pallecchi, M. Codda, D. Marré, C. Cantoni, J. Gazquez, M. Varela, S. J. Pennycook, and F. M. Granozio, Appl. Phys. Lett. **97**, 152111 (2010).
[21]C. Li, Q. Xu, Z. Wen, S. Zhang, A. Li, and D. Wu, Appl. Phys. Lett. **103**, 201602 (2013).
[22]P. Blaha, K. Schwarz, G. K. Madsen, D. Kvasnicka, and J. Luitz, "*An Augmented Plane Wave Plus Local Orbitals Program for Calculating Crystal Properties*" (Vienna University Technology, 2001).
[23]T. R. Paudel and E. Y. Tsymbal, Phys. Rev. B **96**, 245423 (2017).
[24]M. Salluzzo, J. C. Cezar, N. B. Brookes, V. Bisogni, G. M. De Luca, C. Richter, S. Thiel, J. Mannhart, M. Huijben, A. Brinkman, G. Rijnders, and G. Ghiringhelli, Phys. Rev. Lett. **102**, 166804 (2009).
[25]F. Trier, D. V. Christensen, and N. Pryds, J. Phys. Appl. Phys. **51**, 293002 (2018).
[26]A. Kalabukhov, R. Gunnarsson, J. Börjesson, E. Olsson, T. Claeson, and D. Winkler, Phys. Rev. B **75**, 121404 (R) (2007).
[27]S. Y. Moon, C. W. Moon, H. J. Chang, T. Kim, C.-Y. Kang, H.-J. Choi, J.-S. Kim, S.-H. Baek, and H. W. Jang, Electron. Mater. Lett. **12**, 243 (2016).
[28]J. Biscaras, S. Hurand, C. Feuillet-Palma, A. Rastogi, R. C. Budhani, N. Reyren, E. Lesne, J. Lesueur, and N. Bergeal, Sci. Rep. **4**, 6788 (2015).
[29]S. Gariglio, A. Fête, and J.-M. Triscone, J. Phys.: Condens. Matter **27**, 283201 (2015).
[30]L. Yu and A. Zunger, Nat. Commun. **5**, 5118 (2014).
[31]Y. Z. Chen, N. Bovet, F. Trier, D. V. Christensen, F. M. Qu, N. H. Andersen, T. Kasama, W. Zhang, R. Giraud, J. Dufouleur, T. S. Jespersen, J. R. Sun, A. Smith, J. Nygård, L. Lu, B. Büchner, B. G. Shen, S. Linderoth, and N. Pryds, Nat. Commun. **4**, 1371 (2013).
[32]G. Drera, G. Salvinelli, A. Brinkman, M. Huijben, G. Koster, H. Hilgenkamp, G. Rijnders, D. Visentin, and L. Sangaletti, Phys. Rev. B **87**, 075435 (2013).
[33]E. Slooten, Z. Zhong, H. J. A. Molegraaf, P. D. Eerkes, S. de Jong, F. Massee, E. van Heumen, M. K. Kruize, S. Wenderich, J. E. Kleibeuker, M. Gorgoi, H. Hilgenkamp, A. Brinkman, M. Huijben, G. Rijnders, D. H. A. Blank, G. Koster, P. J. Kelly, and M. S. Golden, Phys. Rev. B **87**, 085128 (2013).
[34]S. Nemšák, G. Conti, G. K. Palsson, C. Conlon, S. Cho, J. E. Rault, J. Avila, M.-C. Asensio, C. A. Jackson, P. Moetakef, A. Janotti, L. Bjaalie, B. Himmetoglu, C. G. Van de Walle, L. Balents, C. M. Schneider, S. Stemmer, and C. S. Fadley, Appl. Phys. Lett. **107**, 231602 (2015).
[35]P. Xu, Y. Ayino, C. Cheng, V. S. Pribiag, R. B. Comes, P. V. Sushko, S. A. Chambers, and B. Jalan, Phys. Rev. Lett. **117**, 106803 (2016).
[36]M. Takizawa, S. Tsuda, T. Susaki, H. Y. Hwang, and A. Fujimori, Phys. Rev. B **84**, 245124 (2011).
[37]A. Koitzsch, J. Ocker, M. Knupfer, M. C. Dekker, K. Dörr, B. Büchner, and P. Hoffmann, Phys. Rev. B **84**, 245121 (2011).
[38]M. Sing, G. Berner, K. Goß, A. Müller, A. Ruff, A. Wetscherek, S. Thiel, J. Mannhart, S. A. Pauli, C. W. Schneider, P. R. Willmott, M. Gorgoi, F. Schäfers, and R. Claessen, Phys. Rev. Lett. **102**, 176805 (2009).